



Research article

Regulatory effect of long-stranded non-coding RNA-CRNDE on neurodegeneration during retinal ischemia-reperfusion

Ting-Ting Sun^{a,b,1,2}, Xiu-Miao Li^{a,b,1,2}, Jun-Ya Zhu^{a,b,1,2}, Wen Yao^{a,b,1,2}, Tian-Jing Yang^{a,b,1,2}, Xiang-Rui Meng^c, Jin Yao^{a,b,**}, Qin Jiang^{a,b,*}^a The Affiliated Eye Hospital, Nanjing Medical University, Nanjing, China^b The Fourth School of Clinical Medicine, Nanjing Medical University, Nanjing, China^c Faculty of Art and Science, Queens University, Kingston, Ontario, Canada

ARTICLE INFO

Keywords:

Retinal ischemia-reperfusion injury

Long non-coding RNA

Retinal neurodegeneration

ABSTRACT

Ischemia/reperfusion (I/R) injury is a common pathological mechanism involved in many ocular diseases. I/R is characterized by microvascular dysfunction and neurodegeneration. However, the mechanisms of neurodegeneration induced by I/R remain largely unknown. This study showed that the expression of long non-coding RNA-CRNDE was significantly upregulated after retinal ischemia-reperfusion (RIR). lncRNA-CRNDE knockdown alleviated retinal neurodegeneration induced by RIR injury, as shown by decreased reactive gliosis and reduced retinal cells loss. Furthermore, lncRNA-CRNDE knockdown directly regulated Müller cell function and indirectly affected RGC function *in vitro*. In addition, lncRNA-CRNDE knockdown led to a significant reduction in the release of several cytokines after RIR. This study suggests that lncRNA-CRNDE is a promising therapeutic target for RIR.

1. Introduction

Retinal ischemia-reperfusion (RIR) is a major pathological process contributing to permanent visual impairment and blindness associated with multiple ocular diseases, such as age-related macular degeneration, diabetic retinopathy, glaucoma, retinal vein occlusion, and retinopathy of prematurity [1]. Current treatments of RIR mainly focus on arresting disease progression using intraocular anti-angiogenic vascular endothelial growth factor (VEGF) injections, angiostatic steroids and anti-inflammatory eye drops, or surgery [2, 3, 4]. However, the retinal neuroprotective effects of these therapeutic approaches are limited by the fact that these treatments only target late-stage pathology. It is reported that RIR injury is characterized by sequential events of reactive oxygen species (ROS), leukocyte aggregation, inflammatory response, intracellular calcium overload, glutamate-induced excitotoxic damage, and retinal neurodegeneration [5, 6, 7]. Nevertheless, various underlying physiological and pathological mechanisms contributing to RIR injury need further elucidation. Consequently, these new insights may provide

us with new clinically effective therapeutic methods for many retinal diseases.

Long non-coding RNAs (lncRNAs) have been identified as non-coding transcripts of longer than 200 nucleotides that do not harbor protein-coding signatures [8]. Growing evidence has revealed that lncRNAs may function as the novel gene expression moderators, playing a pivotal role in the various biological processes, such as cell cycle, cell differentiation, epigenetic regulation, and tissue homeostasis [9]. Recent studies have shown that aberrant lncRNA expression is implicated in multiple human diseases ranging from neurodegenerative diseases to cancers. Furthermore, the homeostasis and plasticity of neuronal signaling are required for sophisticated gene regulatory mechanisms [10]. Given the important roles of lncRNAs in gene regulation and tissue homeostasis, the findings suggest that lncRNAs play critical roles in neurodegeneration in RIR injury.

Colorectal neoplasia differentially expressed (CRNDE) is located on the long arm of chromosome 16 of the human genome. Although first identified as a novel lncRNA gene in human colorectal cancer [11], it was upregulated in multiple neoplastic tissues, such as colorectal cancer,

* Corresponding author.

** Corresponding author.

E-mail addresses: dryaojin@vip.sina.com (J. Yao), jqin710@vip.sina.com (Q. Jiang).¹ These authors contributed equally to this work.² T-TS, X-ML, J-YZ, W-Y and T-JY contributed equally to the work presented here and should therefore be regarded as equivalent authors.

renal cell carcinoma, breast cancer, and glioma. Indeed, subsequent analysis revealed that CRNDE is the most upregulated lncRNAs in glioblastoma multiforme. It was found that lncRNA-CRNDE could regulate the tumor cells' proliferation, invasion, metastasis, and cellular pluripotency via specific pathways [12]. Besides cancer progression, lncRNA-CRNDE is involved in fundamental processes of hypoxic-ischemic brain damage, and its expression level is increased in a time-dependent manner. This study also suggested lncRNA-CRNDE silencing alleviated ischemic brain injury [13]. The retina and optic nerve develop as a direct extension of the diencephalon in the course of embryonic development. As a result, the brain and eye share several characteristics, including similar microvasculature and many underlying gene regulatory networks. Thus, lncRNA-CRNDE may play a functional role in the pathogenesis of RIR injury. In the present study, we constructed a mouse RIR model to investigate the expression pattern of lncRNA-CRNDE, and evaluated the effect of CRNDE silencing *in vivo* and *in vitro*. Our study demonstrated that lncRNA-CRNDE expression was significantly upregulated after RIR. lncRNA-CRNDE silencing alleviated retinal neurodegeneration induced by RIR injury, as shown by decreased reactive gliosis and reduced retinal cells loss *in vivo*. lncRNA-CRNDE silencing directly regulated Müller cell function and indirectly affected RGC function *in vitro*. lncRNA-CRNDE knockdown led to a significant reduction in the release of several cytokines after RIR. This study provides novel insights into the molecular mechanisms of RIR injury and suggests that lncRNA-CRNDE could serve as a therapeutic target for RIR.

2. Materials and methods

2.1. Animal preparation and ethics statement

All animal experiments performed in this study followed the guidelines of the ARVO Statement for the Use of Animals in Ophthalmic and Vision Research and approved by the Animal Ethics and Experimentation Committee of Nanjing Medical University (NJMUEC-2018-28). Four-week-old C57BL/6J male mice (supplied by the Experimental Animal Center of Nanjing Medical University, China) were fed a standard diet, provided water randomly, and housed in a 12-h light/12-h dark cycle.

2.2. Induction of RIR model

The RIR model was induced as previously described [14]. Briefly, mice were anesthetized with an intraperitoneal injection of a mixture of ketamine (80 mg/kg) and xylazine (4 mg/kg). Pupils were dilated with 0.5% tropicamide and 2.5% phenylephrine (Mydrin-P; Santen, Osaka, Japan) followed by a few drops of topical anesthetic 0.4% oxybuprocaine hydrochloride (Benoxil; Santen, Osaka, Japan) on the ocular surface. For retinal ischemia, the anterior chamber was cannulated with a 30-gauge infusion needle connected by silicone tubing to a reservoir of sterile 0.9% saline, and intraocular pressure (IOP) increased to 90 mmHg. The needle was pulled out carefully 45 min later, and the retinal blood supply was restored after reperfusion. The sham operation, which served as the control, was performed without elevating the IOP. The animals were excluded if the cornea, iris and lens were injured during puncture, if the puncture needle slipped out during anterior chamber pressor perfusion, or if the retinal ischemia did not last for 45 min. After surgery, tobramycin ointment (Alcon, USA) was applied to prevent bacterial infections. Eyes were processed after 6h, 1,3, or 7 days postinjury.

2.3. Intravitreal injection

Total mice were randomly divided into 4 groups (4 animals/group), (1) normal control group; (2) RIR group; (3) RIR + scrambled (Scr) small hairpin (shRNA) group; (4) RIR + CRNDE shRNA. Random numbers were generated using an online random order generator (<https://www.graphpad.com/quickcalcs/randomize1/>). All mice were anesthetized before intravitreal injection by pupil dilation with 0.5% tropicamide and 2.5%

phenylephrine. The adeno-associated virus (AAV) solution (2 μ L, 10^{12} v. g/ml) loaded with CRNDE shRNA or Scr shRNA was delivered into the vitreous using a 33-gauge needle four weeks before the onset of reperfusion to maximize the transfection efficiency. CRNDE shRNA targeting sequence was 5'- TCCCTTACCTCACCTGGATCTCTT -3' and Scr shRNA targeting sequences was 5'- TTCTCCGAACGTGTCCACGT -3'.

2.4. Electroretinogram (ERG) measurements

On the seventh day after RIR injury, retinal function was monitored using full-field flash electroretinography. C57BL/6J male mice were maintained in the complete darkness overnight before the ERG recording session. Mice were anesthetized with ketamine (80 mg/kg) and xylazine (4 mg/kg), and the pupils were dilated with topical 0.5% tropicamide and 2.5% phenylephrine before recording. Then, 0.4% oxybuprocaine hydrochloride was applied to topically anesthetize the corneas before a Gold-plated wire loop contact lens electrode was placed on the tested eye. The full-field flash ERG was recorded using custom DTL fiber electrodes with an Espion testing system and ColorDome LED/Xenon-full field stimulator (Diagnosys LLC, Lowell, MA). Stainless steel needle electrodes were inserted into the skin between the two ears and into the base of the tail, serving as reference and ground leads, respectively. After completing a scotopic intensity series, photopic flash responses were recorded in the presence of an adapting white light. Flash ERG records were bandpass filtered at 0.3 and 500 Hz. The amplitude of the a-wave and b-wave was measured by the Roland Consult Color Ganzfeld Q450C recording machine.

2.5. Immunofluorescence analysis of retinal sections

Seven days after RIR, eyes were enucleated and processed for immunohistology. For immunohistology, the eyeballs were fixed in 4% paraformaldehyde (PFA) overnight, two days of incubated in 30% sucrose, embedded in OCT compound (Thermo Scientific, 6502), and stored at -80°C . The tissue was then sectioned into 10- μ m-thick slices by a cryostat (Thermo Fisher Scientific, Walldorf, Germany). Immunofluorescent analysis was performed as previously described [15]. The retinal cross-sections were first dried and rehydrated in PBS. Retinal sections were permeabilized with 0.5% Triton X-100 for 30 min and then blocked with 10% bovine serum albumin (BSA) for 30 min. Six retinal sections per eye were used for each staining. Tissues were incubated with the appropriate primary antibodies at 4°C overnight for each staining. Subsequently washed with PBS, retinal sections were incubated with fluorophore-conjugated secondary antibodies for 3 h at room temperature (Table 1). RGCs, amacrine cells, horizontal cells, bipolar cells, microglia, Müller cells, and photoreceptor cells were labeled using specific antibodies. Finally, cell nuclei were stained with 4',6-diamidino-2-phenylindole (DAPI, Beyotime, c1002). The retinal sections were observed using an Olympus IX-73 microscopy, and the fluorescent signals were analyzed by ImageJ.

2.6. Quantitative real-time PCR analysis

For qRT-PCR analyses, the retina was dissected out, snap-frozen in a lysis buffer with TRIzol reagent (Life Technologies, 15596026) in liquid nitrogen, and stored at -80°C until RNA extraction. The quality and purity of RNA were detected spectrophotometrically. cDNA was converted from total RNA using Prime Script RT Master Mix (Takara, RR036A) according to the manufacturer's instructions. Quantitative real-time PCR was performed with SYBR Green (Thermo Fisher Scientific, 100029284), and the data collection was performed on the PikoReal Real-Time PCR System (Thermo Scientific). The primers were synthesized by Gene Pharma (Shanghai, China). The relative expression level of indicated genes (lnc-CRNDE, ICAM-1, IL-6, TNF- α , and Rpl13a) was compared with that of Rpl13a, and expression fold changes were calculated using $2^{-\Delta\Delta\text{Ct}}$ methods [16]. The primer sequences of different genes are tabulated in Table 2.

Table 1. List of used primary and secondary antibodies, including cell type, dilution, and company.

Primary antibody	Cell type	Dilution	Company	Secondary Antibody with Dilution	Company
NeuN	RGCs	1:400	Abcam, ab177487	Alexa Fluor 594 Goat anti-rabbit, 1:500	Invitrogen
GFAP	Glia	1:200	Abcam, ab68428	Alexa Fluor 594 Goat anti-rabbit, 1:200	Invitrogen
GS	Müller cells	1:400	Abcam, ab228590	Alexa Fluor 594 Goat anti-rabbit, 1:500	Invitrogen
PKC α	Bipolar cells	1:400	Abcam, ab32376	Alexa Fluor 488 Goat anti-rabbit, 1:500	Invitrogen
Calretinin	Amacrine cells	1:200	Santa Cruz, sc-365956	Alexa Fluor 594 Goat anti-mouse, 1:500	Invitrogen
Calbindin	Horizontal cells	1:200	Santa Cruz, sc-365360	Alexa Fluor 594 Goat anti-mouse, 1:500	Invitrogen
Rhodopsin	Photoreceptor cells	1:400	Abcam, ab5417	Alexa Fluor 594 Goat anti-rabbit, 1:500	Invitrogen
Iba-1	microglia	1:100	HuaBio, ET1705-78	Alexa Fluor 594 Goat anti-rabbit, 1:500	Invitrogen

2.7. Hematoxylin and eosin (HE) staining

For histological analysis, the eyeballs were fixed in 4% paraformaldehyde (PFA, Biosharp Biotechnology, BL539A) overnight at 4 °C, paraffin embedded, and sectioned (6 μ m thick). Three sections per eye were stained with HE to obtain a structural overview of the retinal layers. After the HE staining, all slides were dehydrated in ethanol and then incubated in xylene before being mounted with neutral balsam (Biosharp, 69070060) and observed under an Olympus IX-73 microscope. For each analysis, values were measured in triplicates and averaged.

2.8. Cell culture and transfection

Primary Müller cells were isolated from mice at postnatal day 7. Briefly, eyeballs were incubated in serum-free media overnight. Retinas were enzymatically incubated with trypsin (0.25%)/collagenase (65U/mL) at 37 °C for 20 min, and then rinsed in Dulbecco's modified Eagle medium (DMEM, Gibco, C11995500BT) containing 10% fetal bovine serum (FBS, Gibco, 10099141) to terminate digestion. Retinas were dissected into small aggregates from the remaining tissue and plated in primary Müller glia cell culture media: DMEM-high glucose, without L-glutamine, with sodium pyruvate +1% GlutaMax, 1% Penicillin/Streptomycin, and 10% FBS. The isolated cells became confluent after the cultures had been maintained for 7–10 days. The third passaged cells were used for the subsequent experiments, and cultured cells were identified using the antibodies against the glial fibrillary acidic protein (GFAP) and glutamine synthetase (GS).

Primary RGCs were isolated and cultured according to the two-step immunopanning protocol. Retinas were collected from C57BL/6J mouse pups at postnatal day 0–3 and dissociated in papain solution (15 U/mL) and collagenase (70 U/mL) for 15 min. Subsequently, retina cell suspensions were incubated with antimacrophage antiserum antibody-coated flasks to remove adherent macrophages and microglial cells. Non-adherent cells were incubated with mouse Thy1.2 monoclonal antibody to purify RGCs. The purity of the primary RGCs in cultures were determined by staining with the antibody Tuj1 (Abcam, ab18207), specific RGCs markers. Primary RGCs were cultured in serum-free Neurobasal-A medium (Gibco) supplemented with penicillin, streptomycin, 25

ng/mL CNTF, 25 ng/mL BDNF, 10% FBS, 10 mM forskolin, and B27. All cultures were incubated at 37 °C, in 5% CO₂, and with 95% relative humidity. Müller cells were transfected using Lipofectamine 2000 (Life Technologies, 13778150) with three small interfering RNAs (siRNAs; Gene Pharm) targeting lncRNA-CRNDE according to the manufacturer's protocol, and the transfection efficiencies of three CRNDE siRNAs were 77.2%, 34.1% and 37.1%, respectively (Figure 5B). The siRNA target sequence was shown as follows (Table 3):

2.9. Cell proliferation assay

Cell proliferation was determined using 5-ethynyl-2'-deoxyuridine (EdU) DNA Cell Proliferation kit (Beyotime, C0071S) following the manufacturer's protocol. After the required treatment, cells were incubated with 1 \times EdU working liquid for 2 h and then fixed in 4% PFA for 15 min. After washing, cells are blocked with 0.3% Triton X-PBS for 15 min and then incubated with click reaction liquid for 30 min at room temperature in the dark. The cells were finally mounted using the anti-fade medium containing 1 \times Hoechst 33342 (Beyotime, C0071S) and observed under an Olympus IX-73 microscope.

2.10. 3-(4,5-Dimethylthiazol-2-yl)-2,5-diphenyltetrazolium bromide (MTT) assay

The MTT assay was used to measure the viability of the cells. Briefly, Müller Cells (1 \times 10⁴) were plated in each well of a 96-well plate and allowed to adhere for 24 h. After specific treatment, 30 μ L of 0.5 mg/mL MTT (BioFroxx, 1334GR001) (in PBS) was added to each well and incubated for an additional 3 h at 37 °C. After discharging the medium, 200 μ L DMSO/well was added to the culture cells to dissolve formazan crystals [17]. The absorbance value in each well was measured at the wavelength of 595 nm using a microplate reader (Molecular Devices).

2.11. Rhodamine 123 staining

Rhodamine123 assays were performed to determine the DNA condensation and nuclear fragmentation. After the required treatment, cells were incubated with the 10 μ mol/L rhodamine123 (Solarbio, R8030) at 37 °C for 1.5 h in the dark. The fluorescence intensity of harvested cells was detected using an Olympus IX-73 microscope.

Table 2. Primer sequences for real-time PCR.

Primer sequence		
lncRNA-CRNDE for mice	Forward	5'-CTCTGGTCCAGGACGAAGACT-3'
	Reverse	5'-CCTTTGCACTCGATGGGAAC-3'
ICAM-1 mRNA for mice	Forward	5'-GGAAGGGAGCCAAGTAAGTGTGAAG-3'
	Reverse	5'-GAGCGGCAGAGCAAAGAAGC-3'
IL-6 mRNA for mice	Forward	5'-TCCATCCAGTTGCCTTCTTG-3'
	Reverse	5'-TTCCACGATTTCCAGAGAAC-3'
TNF- α mRNA for mice	Forward	5'-CTTCTG TCTACTGAACITCGGG-3'
	Reverse	5'-CAGGCTTGTCACCTCGAATTTTG-3'
Rpl13a mRNA for mice	Forward	5'-AGCCTACCAGAAAGTTTGCTTAC-3'
	Reverse	5'-GCTTCTTCTCCGATAGTGATC-3'

Table 3. siRNA sequences for CRNDE.

siRNA sequence		
CRNDE siRNA1	sense	5'-GGUGGAAGGAGGUGAUUUUATT-3'
	antisense	5'-UAAAUCACCUCCUCCACCTT-3'
CRNDE siRNA2	sense	5'-CACCUCUUUAAAUCUUGAUTT-3'
	antisense	5'-AUCAAGAUUUAAAAGAGGUGTT-3'
CRNDE siRNA3	sense	5'-CAUCCACACACAUACAAUATT-3'
	antisense	5'-UUAUGUAUGUGUGGAUUTT-3'
Scr siRNA	sense	5'-UUCUCCGAACGUGUCACGUTT-3'
	antisense	5'-ACGUGACACGUUCGGAGAATT-3'

2.12. *In vitro* oxygen glucose deprivation/reoxygenation (OGD/R)-induced cell damage

To mimic the murine model of RIR, primary Müller cells and RGCs were subjected to oxygen-glucose deprivation for 6 h and subsequently returned to normal environment for 12 h. Specifically, cells were cultured in glucose-free medium containing 0.2% FBS and 1% penicillin/streptomycin in a hypoxia chamber (95% N₂ and 5% CO₂) for 6 h after transfection. Cells were then shifted to DMEM-high glucose (4.5 g/L), supplemented with 10% FBS and reoxygenated in normoxic conditions (95% air, 5% CO₂) for 12 h. Normoxia control cells were maintained in complete media under normoxic conditions.

2.13. Propidium iodide (PI)/calcein-acetoxymethyl (Calcein-AM) staining

Calcein-AM staining and PI double staining were used to discriminate between viable and dead cells. Cells were stained with a mixture of 10 μmol/L Calcein-AM solutions (AAT Bioquest, 22002), 10 μmol/L PI (Biofroxx, 1246MG100), and 3 μM Hoechst 33342 (Biofroxx, 2289MG025) for 15 min at 37 °C in the dark. After washing with PBS three times, images of live cells (green) and dead cells (red) were captured using a fluorescent microscope. The average percentage of PI-positive cells was counted using the Image J software.

2.14. Hoechst staining

Hoechst 33342 fluorescent dye was used to detect DNA condensation and nuclear fragmentation. After the required treatment, these cells were washed with PBS three times and fixed with 4% PFA for 15 min at room temperature. Subsequently, cells were washed with PBS and then stained with Hoechst 33342 (Biofroxx, 2289MG025) for 15 min. Finally, these stained cells were observed using an Olympus IX-73 microscope.

2.15. Enzyme-linked immunosorbent assay (ELISA)

Mice were anesthetized with intraperitoneal injection of a mixture of ketamine (80 mg/kg) and xylazine (4 mg/kg), and then euthanized by intraperitoneal injection of sodium barbiturate (100 mg/kg). Then retinal tissue was collected and the samples of all groups were kept at 4 °C for biochemical assay. Biochemical indexes were determined using commercial reagent kits (Abcam, UK) according to the manufacturer's instructions. The indirect ELISA assay determined the concentrations of TNF-α, IL-6, and ICAM-1 in the medium of retinal tissue. A microplate

reader measured the optical density (OD) values were measured at 450 nm by a microplate reader.

2.16. Statistical analysis

Data analysis was performed using GraphPad Prism 8 (GraphPad Software, San Diego, CA). All results are expressed as means ± SEM. For the normally distributed data with equal variance, the significant difference was determined by one-way ANOVA to test the effect of group followed by post-hoc Bonferroni's test (when >2 groups were compared). $P < 0.05$ was considered statistically significant.

3. Results

3.1. lncRNA-CRNDE is aberrantly expressed during RIR injury in vivo and OGD/R injury in vitro

A previous study revealed that lncRNA-CRNDE expression levels are significantly upregulated in ischemia-reperfusion injury [18]. Here, we further determined whether RIR injury influenced lncRNA-CRNDE expression *in vivo* and *in vitro*. The rodent RIR model is a well-established animal model which resembles human acute retinal artery occlusion such as CRAO or acute ocular hypertension such as glaucoma. To test whether retinal lncRNA-CRNDE expression level altered in response to RIR injury, eyes were collected at 6 h, 24 h, 3 d, 7 d, and qPCR analysis demonstrated increased lncRNA-CRNDE expression in RIR retinas (Figure 1A). In the RIR model, the circulatory disorder of the retina is induced by elevating the IOP for a definite period. Induced high IOP causes compressed retinal blood vessels and impaired blood flow. The following natural reperfusion induces excessive oxidative stress. Our preliminary results showed that CRNDE was mainly expressed in retinal endothelial cells and Müller cells (data not shown). It is reported that OGD/R is a classical *in vitro* model of RIR [5, 19]. Müller cells were subjected to glucose free media in hypoxia condition to mimic the ischemic phase of I/R, and then returned to normoxia and normal media to mimic the reperfusion phase of I/R. qRT-PCR revealed that lncRNA-CRNDE expression was significantly upregulated in Müller cells subjected to OGD/R (Figure 1B). Collectively, these results indicate that lncRNA-CRNDE is potentially involved in RIR injury.

3.2. lncRNA-CRNDE regulates RIR injury in vivo

To evaluate the effect of lncRNA-CRNDE in RIR injury, lncRNA-CRNDE was knocked down in retinas before the onset of retinal

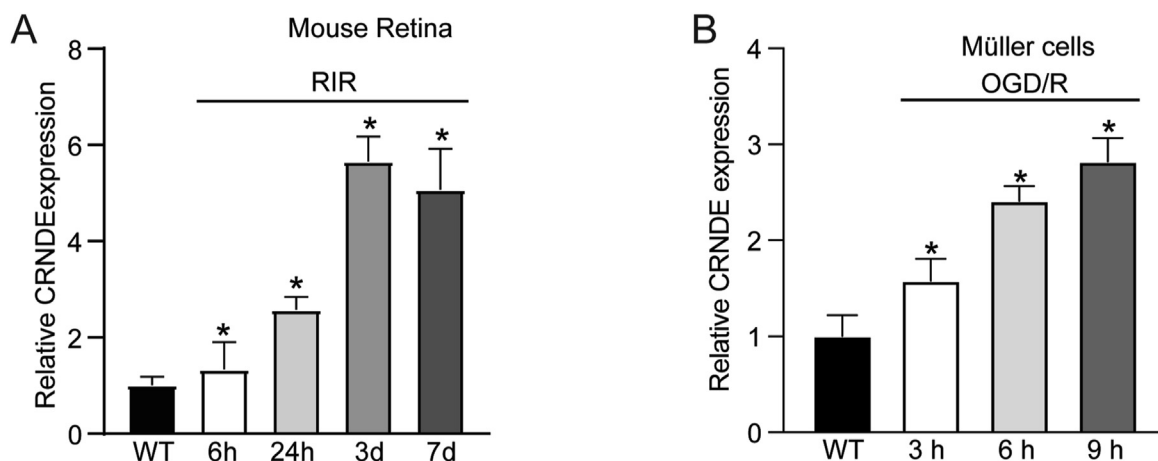
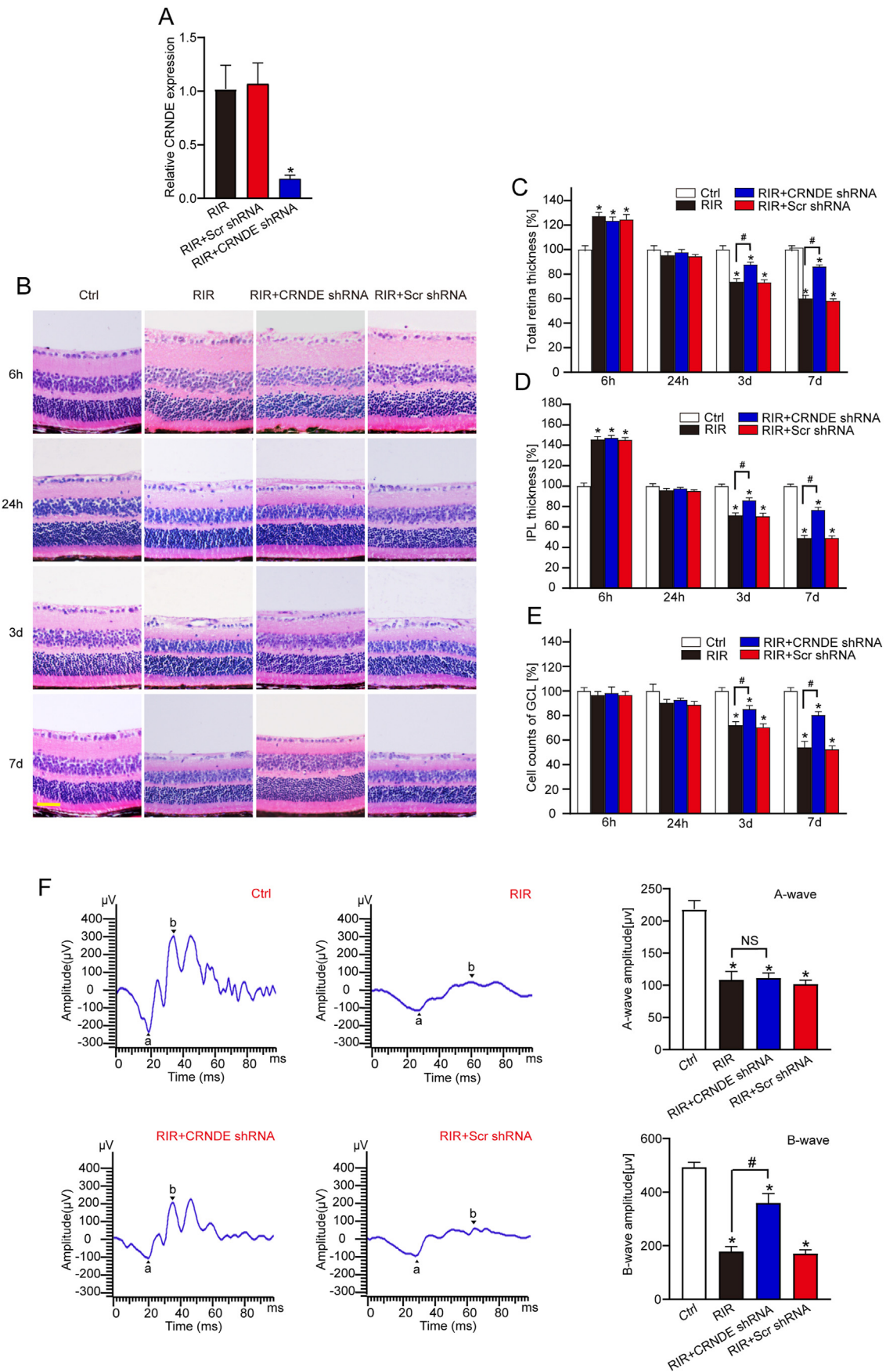


Figure 1. The expression pattern of long non-coding RNA-CRNDE *in vivo* and *in vitro*. A. Quantitative reverse transcription-polymerase chain reactions (qRT-PCRs) were conducted to detect the level of the lncRNA-CRNDE gene in the retinas after retinal ischemia-reperfusion (RIR) for 6 h, 24 h, 3 d, or 7 d in C57BL/6J mice (n = 5). * $P < 0.05$ versus WT, one-way ANOVA followed by the Bonferroni post-hoc test. B. Retinal qRT-PCRs were performed to detect the level of the lncRNA-CRNDE gene in Müller cells after 3 h, 6 h or 9 h of OGD followed by 12 h of R (n = 4). * $P < 0.05$ versus WT, one-way ANOVA followed by Bonferroni's post-hoc test.



(caption on next page)

ischemia. The experiments were divided into four groups, lncRNA-CRNDE silencing group (lncRNA-CRNDE shRNA), Sc shRNA group, RIR group, and untreated group. qRT-PCR showed that CRNDE shRNA injection significantly reduced the levels of CRNDE in the retinas (Figure 2A).

After I/R injury induction, histomorphology of the HE-stained retina was observed (Figure 2B). We found that retinal damage occurred rapidly in mice with retinal edema, vacuolar degeneration, condensation of nuclear chromatin by HE staining as early as 6 h after RIR (Figure 2B). Furthermore, the inner plexiform layer (IPL) thickness, total retina thickness, and cell density in the ganglion cell layer (GCL) were measured after the RIR injury. Regarding these histological features, a distinct degradation of the whole retina started at the 6th hour after RIR, and these changes persisted for seven days (Figure 2B). Furthermore, a significantly reduced thickness of the whole retina and IPL were detected at days 3 and 7 in ischemic eyes compared to the control group. lncRNA-CRNDE shRNA treatment dramatically relieved the damage (Figures 2C, 2D). Consistently, cell counts of GCL decreased after 6 h of RIR, while lncRNA-CRNDE shRNA mice presented no significant difference at this point. Whereas, surviving cells decreased in the GCL of retinas on days 3 and 7 after RIR, which was relieved by lncRNA-CRNDE shRNA (Figure 2E). These results indicated that lncRNA-CRNDE knockdown attenuated progressive retinal thinning and loss of RGCs induced by RIR injury, especially on day 7 after RIR. Considering these results, each group was observed after 7 days of RIR for all studies below.

To further assess retinal function, we employed retinal ERG to detect the effect of lncRNA-CRNDE on visual function. The representative ERG waveforms for each group were shown. The ERG measurements 7 days after RIR showed a significant decrease in the a-wave and b-wave amplitude compared to the control group. Compared with RIR and Sc shRNA mice, the amplitudes of b-wave were increased in the lncRNA-CRNDE shRNA group, but the amplitudes of a-wave were not improved in the lncRNA-CRNDE shRNA group (Figure 2F), suggesting that lncRNA-CRNDE shRNA silencing partially prevents ERG abnormality induced by RIR injury and ameliorate retinal function. These results revealed that lncRNA-CRNDE knockdown could partially alleviate retinal function under RIR injury.

Encouraged by these findings, we further investigated the potential neuroprotective effects of lncRNA-CRNDE in the RIR mice model. RGC degeneration and reactive gliosis are two important features of retinal neurodegeneration under RIR injury. To this end, we performed protein immunolabeling experiments to explore if lncRNA-CRNDE is capable of regulating neuroinflammation, as well as its underlying mechanisms. Müller glia is the major glial component of the retina, and its excessive activation is a general response to injury and inflammation in the damaged retina [20]. As expected, RIR notably increased reactive gliosis as shown by increased GFAP staining and GS staining in the retina. However, aberrant gliosis was inhibited by lncRNA-CRNDE shRNA with lower expression of GFAP and GS, thus exerting protection against RIR injury (Figures 3A, 3B). Meanwhile, current study shows that microglia are the major performer in neuroinflammation, and their activation

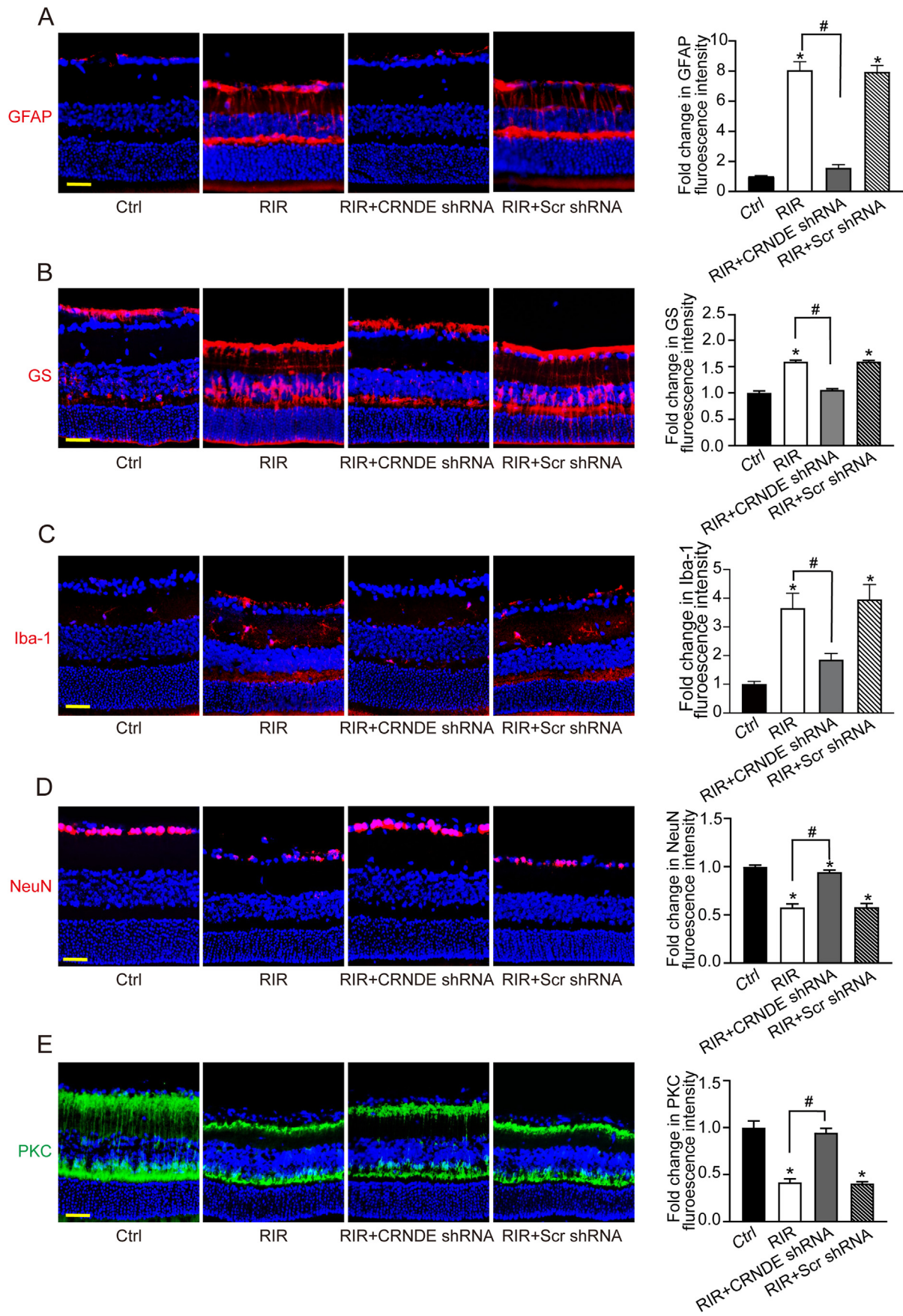
could aggravate retinal disease by releasing several toxic and pro-inflammatory mediators [21]. Immunofluorescence staining of microglial marker Iba-1 showed that RIR injury increased the number of Iba-1+ cells, but lncRNA-CRNDE silencing reduced this trend (Figure 3C). Moreover, RIR injury caused a marked decrease in RGC number as shown by decreased NeuN (the specific marker of RGCs), which was mostly prevented in lncRNA-CRNDE shRNA retinas as shown by the increased number of NeuN-positive RGCs. The positive signals located in the GCL suggested the presence of live RGCs. Thus, lncRNA-CRNDE silencing may have a beneficial effect on facilitating RGC survival, as shown by increased NeuN staining (Figure 3D).

The ERG measurements showed a functional disorder of the cells in the inner nuclear layer (INL) 7 days after ischemia induction. Accordingly, we examined those cells in the next step. In the normal retina, bipolar cells extend throughout the IPL, INL, and OPL [22]. Anti-PKC α was used to visualize bipolar cells [23]. The immunolabeling showed a progressive diminution of PKC α + cells in the RIR retina, whereas lncRNA-CRNDE shRNA prevented the reduction in the PKC α positive bipolar cells (Figure 3E). In the normal retina, starburst amacrine cells distribute in the GCL and the innermost side of the INL, and their dendrites stratify into two distinct layers in the IPL [24]. Compared with RIR retinas, lncRNA-CRNDE shRNA protected RGCs as shown by the increased number of calretinin-labeled cells in the GCL, while lncRNA-CRNDE shRNA allowed no significant retention of amacrine cells (calretinin-labeled cells in the INL) (Figure 4A). Moreover, RIR caused observable changes in horizontal cells. However, lncRNA-CRNDE shRNA did not further affect the number of calbindin labeled horizontal cells compared with RIR retinas (Figure 4B). Similarly, rhodopsin immunolabeling revealed that lncRNA-CRNDE shRNA did not affect photoreceptors (rod cells) compared with noticeable changes in RIR injury (Figure 4C). Collectively, these results indicate that lncRNA-CRNDE affects reactive retinal gliosis and the survival of RGCs and bipolar cells.

3.3. lncRNA-CRNDE directly affects müller glial cell function and indirectly affects RGC function in vitro

The above mentioned results showed that lncRNA-CRNDE is mainly expressed in Müller cells and RGCs. Primary Müller cells were cultured and identified with GFAP and GS antibodies, the result showed that the percentage of GFAP+/GS+ cells was more than 90% (Figure 5A). Next, OGD/R was conducted to determine the role of lncRNA-CRNDE on Müller cells and RGCs function *in vitro*. We designed three different CRNDE siRNAs, and qPCR analysis revealed that all CRNDE siRNAs could significantly reduce CRNDE expression levels in Müller cells (Figure 5B). We selected CRNDE siRNA1 for the subsequent experiments due to its higher silencing efficiency. We observed that lncRNA-CRNDE knockdown further reduced Müller cells viability treated with OGD/R (Figure 5C). EdU immunofluorescence staining showed that lncRNA-CRNDE knockdown significantly decreased the proliferation of Müller cells compared with the OGD/R group (Figure 5D). We then determined whether lncRNA-CRNDE regulates the development of OGD/R-induced

Figure 2. lncRNA-CRNDE knockdown ameliorates retinal function after retinal ischemia-reperfusion. A. Mice received an intravitreal injection of Sc shRNA, CRNDE shRNA, or left untreated (Ctrl). qRT-PCRs were conducted to detect CRNDE levels in retinal tissue (n = 3). B. HE staining of C57BL/6J retinas treated with an intravitreal injection of Sc shRNA or lncRNA-CRNDE shRNA or left untreated after four weeks exposed to IOP of 90 mmHg for 6 h, 24 h, 3 d, or 7 d (n = 3). C. A significant decrease of the total retinal thickness was measured in ischemic eyes starting at day three after RIR. lncRNA-CRNDE knockdown ameliorated the attenuation of total retinal thickness induced by RIR (3 days, 7 days). * $P < 0.05$, significant difference compared with the Ctrl nonischemic group. # $P < 0.05$, significant difference compared with the RIR groups. The significant difference was determined by one-way ANOVA followed by the Bonferroni test. D. Retinas exposed to RIR injury displayed a significant decrease in IPL thickness starting at day three. lncRNA-CRNDE knockdown ameliorated the attenuation of IPL thickness induced by RIR (3 days, 7 days). * $P < 0.05$, significant difference compared with the Ctrl nonischemic group. # $P < 0.05$, significant difference compared with the RIR group. The significant difference was determined by one-way ANOVA followed by the Bonferroni test. E. The cell survival rate of GCL was significantly decreased in response to RIR injury, which was prevented by lncRNA-CRNDE knockdown (3 days, 7 days: $p < 0.05$). GCL, ganglion cell layer; IPL, inner plexiform layer; scale bar: 20 μm * $P < 0.05$, significant difference compared with the Ctrl nonischemic group. # $P < 0.05$, significant difference compared with the RIR groups. The significant difference was determined by one-way ANOVA followed by the Bonferroni test. F. Seven days after RIR induction, ERG was recorded in nonischemic mice (Ctrl), RIR mice, Ad-Sc shRNA-injected, and Ad-CRNDE shRNA-injected RIR mice. The representative ERGs are shown. In addition, amplitudes of a and b waves were statistically analyzed (n = 4). * $P < 0.05$, significant difference compared with the Ctrl nonischemic group. # $P < 0.05$, significant difference compared with the RIR groups. The significant difference was determined by one-way ANOVA followed by the Bonferroni test.



(caption on next page)

Figure 3. lncRNA-CRNDE knockdown affects reactive retinal gliosis and RGC survival *in vivo*. C57BL/6J mice (4-week-old, male) received an intravitreal injection of Scr shRNA or lncRNA-CRNDE shRNA or left untreated. Four weeks after shRNA injection, RIR was induced. The group without RIR served as the control (Ctrl) group. A. Retinal cross-section of 7 days after RIR and retinal cross-section without RIR were immunolabeled with anti-GFAP. The signal was quantified to detect retinal reactive gliosis (GFAP+, red) in all groups. A representative image was shown (n = 3; scale bar: 100 μ m). * P < 0.05, compared with the Ctrl; # P < 0.05, compared with the RIR. The significant difference was determined by one-way ANOVA followed by the Bonferroni test. B. Retinal cross-section of 7 days after RIR and retinal cross-section without RIR were immunolabeled with anti-GS. The signal was quantified to detect Müller cell activation (GS+, red) in all groups. A representative image was shown (n = 3; scale bar: 100 μ m). * P < 0.05, compared with the Ctrl; # P < 0.05, compared with the RIR. The significant difference was determined by one-way ANOVA followed by the Bonferroni test. C. Retinal cross-section of 7 days after RIR and retinal cross-section without RIR were immunolabeled with anti-Iba-1. The signal was quantified to detect activated microglia (Iba-1+, red) in all groups. A representative image was shown (n = 3; scale bar: 100 μ m). * P < 0.05, compared with the Ctrl; # P < 0.05, compared with the RIR. The significant difference was determined by one-way ANOVA followed by the Bonferroni test. D. Retinal cross-section of 7 days after RIR and retinal cross-section without RIR were immunolabeled with anti-NeuN. The signal was quantified to detect surviving RGCs (NeuN+, red) in all groups. A representative image was shown (n = 3; scale bar: 100 μ m). * P < 0.05, compared with the Ctrl; # P < 0.05, compared with the RIR. The significant difference was determined by one-way ANOVA followed by the Bonferroni test. E. Retinal cross-section of 7 days after RIR and retinal cross-section without RIR were immunolabeled with anti-PKC α . The signal was quantified to detect surviving bipolar cells (PKC α +, green) in all groups. A representative image was shown (n = 3; scale bar: 100 μ m). * P < 0.05, compared with the Ctrl; # P < 0.05, compared with the RIR. The significant difference was determined by one-way ANOVA followed by the Bonferroni test.

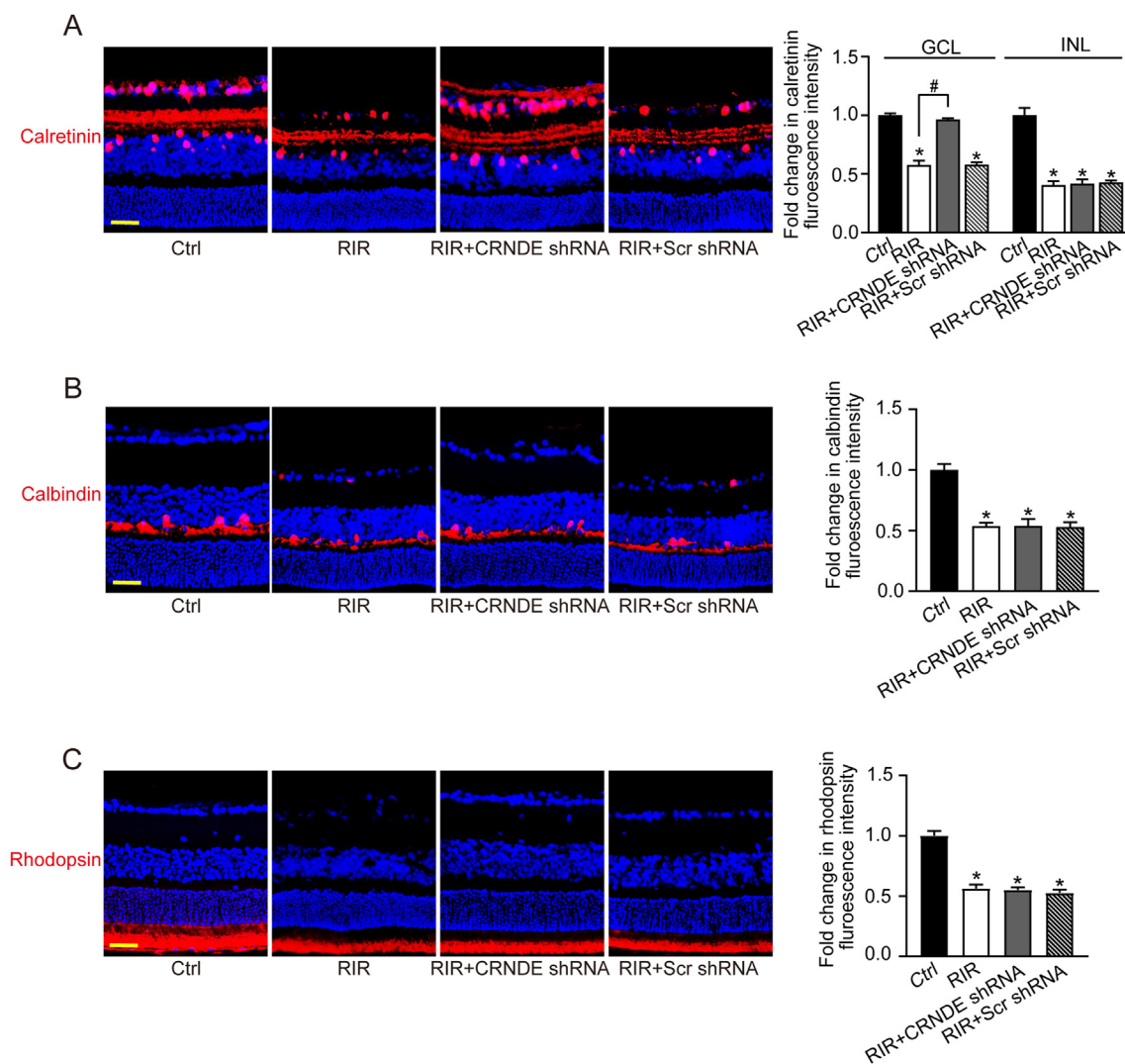


Figure 4. Regularity of expression of optic nerve cells in the retina of RIR mice. C57BL/6J mice (4-week-old, male) received an intravitreal injection of Scr shRNA or lncRNA-CRNDE shRNA or left untreated. Four weeks after shRNA injection, RIR was induced. The group without RIR served as the control (Ctrl) group. A. Retinal cross-section of 7 days after RIR and retinal cross-section without RIR were immunolabeled with anti-Calretinin. The signal was analyzed to quantify the number of amacrine cells (Calretinin+, red) in all groups. A representative image was shown (n = 3; scale bar: 100 μ m). * P < 0.05, compared with the Ctrl; # P < 0.05, compared with the RIR. The significant difference was determined by one-way ANOVA followed by the Bonferroni test. B. Retinal cross-section of 7 days after RIR and retinal cross-section without RIR were immunolabeled with anti-Calbindin. The signal was analyzed to quantify the number of horizontal cells (Calbindin+, red) in all groups. A representative image was shown (n = 3; scale bar: 100 μ m). * P < 0.05, compared with the Ctrl; # P < 0.05, compared with the RIR. The significant difference was determined by one-way ANOVA followed by the Bonferroni test. C. Retinal cross-section of 7 days after RIR and retinal cross-section without RIR were immunolabeled with anti-Rhodopsin. The signal was analyzed to quantify the number of photoreceptor cells (Rhodopsin+, red) in all groups. A representative image was shown (n = 3; scale bar: 100 μ m). * P < 0.05, compared with the Ctrl; # P < 0.05, compared with the RIR. The significant difference was determined by one-way ANOVA followed by the Bonferroni test.

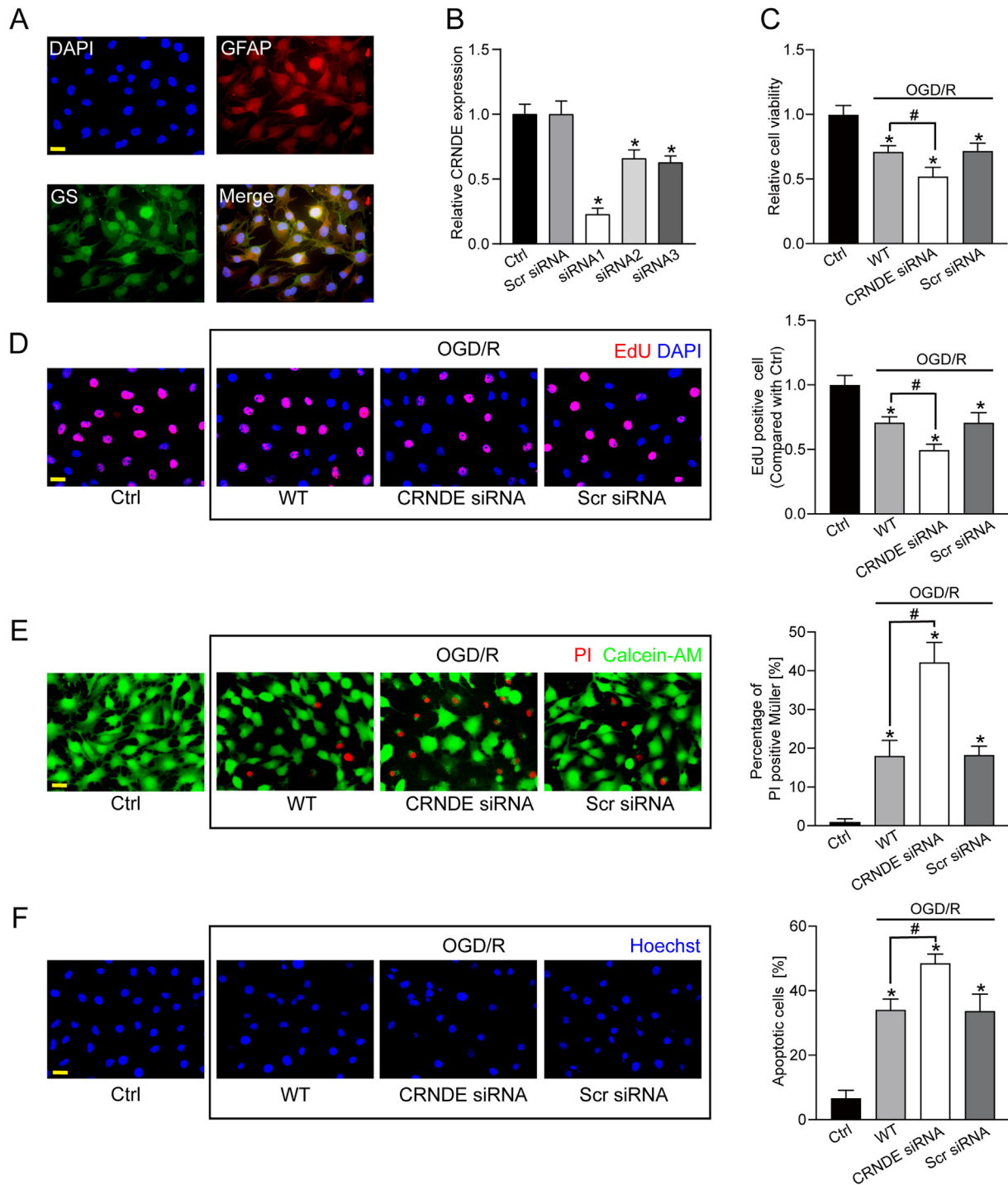


Figure 5. LncRNA-CRNDE knockdown regulates Müller cell function after OGD/R *in vitro*. Primary Müller cells were transfected with Scr siRNA, lncRNA-CRNDE siRNA, or left untreated (WT) and then exposed to OGD (6 h)/R (12 h). The group without any treatment was taken as the control (Ctrl) group. A. Primary Müller cells were confirmed with GFAP and GS antibodies. Blue, DAPI; Red, GFAP; Green, GS (Scale bar: 20 μ m). B. Müller cells were transfected with CRNDE small interfering RNA (siRNA1-3), Scr siRNA, or left untreated (Ctrl) for 48 h. qRT-PCRs were conducted to detect CRNDE expression (n = 4). * $P < 0.05$, compared with the Ctrl. The significant difference was determined by one-way ANOVA followed by Bonferroni test. C. MTT assay and quantification analysis were performed to detect Müller cells viability. All groups were incubated with MTT probe at 37 $^{\circ}$ C for 3 h, then Müller cells viability was detected using microplate reader (n = 4). * $P < 0.05$, compared with the Ctrl; # $P < 0.05$, compared with the WT. The significant difference was determined by one-way ANOVA followed by the Bonferroni test. D. EdU staining and quantification analysis were performed to detect Müller cells proliferation to analyze the incorporation of EdU during DNA synthesis. Blue: nuclei, Red: EdU (n = 4; scale bar: 20 μ m). * $P < 0.05$, compared with the Ctrl; # $P < 0.05$, compared with the WT. The significant difference was determined by one-way ANOVA followed by the Bonferroni test. E. PI/Calcein-AM staining and quantification analysis were performed to detect Müller cells apoptosis. Green, live cells; red, dead, or dying cells (n = 4; scale bar: 20 μ m). * $P < 0.05$, compared with the Ctrl; # $P < 0.05$, compared with the WT. One-way ANOVA determined the significant difference followed by the Bonferroni test. F. Hoechst staining and quantification analysis were performed to detect Müller cells apoptosis observed as apoptotic nuclei (condensed or fragmented) (n = 4; scale bar: 20 μ m). * $P < 0.05$, compared with the Ctrl; # $P < 0.05$, compared with the WT. One-way ANOVA determined the significant difference followed by the Bonferroni test.

apoptosis using Hoechst 33342, PI/Calcein-AM staining. The combination of lncRNA-CRNDE knockdown and OGD/R resulted in a higher apoptotic percentage than OGD/R alone, as shown by more PI-positive cells (dying or dead cells) (Figure 5E) and increased apoptotic nuclei (condensed or fragmented) (Figure 5F). These results suggest that lncRNA-CRNDE silencing decreases the viability and proliferation, and promotes the apoptosis of Müller cells after OGD/R *in vitro*.

To evaluate the effect of Müller cells on RGCs survival when RIR injury occurred, we cultured primary RGCs and performed co-cultures of Müller cells after OGD/R treatment in an approach *in vitro*. Immunofluorescent staining of Tuj1 showed that the percentage of RGCs was about 90% (Figure 6A). MTT assay revealed that co-culture with Müller cells

reduced cells viability, while CRNDE knockdown in Müller cells significantly increased the viability of RGCs (Figure 6B). Immunofluorescent staining results showed that OGD/R shortened the synaptic length of RGCs, co-culture with Müller cell further shortened the synaptic length of RGCs, while CRNDE knockdown in Müller cells obviously alleviated this trend (Figure 6C). Propidium iodide (PI) staining revealed that OGD/R increased apoptotic RGCs, Müller cell co-culture evidently increased the number of apoptotic RGCs, while CRNDE knockdown in Müller cells alleviated this harmful effect (Figure 6D). The above results revealed that the Müller cell co-culture significantly increased the number of apoptotic RGCs induced by OGD/R, and lncRNA-CRNDE knockdown in Müller cells significantly reduced the damaging effect on RGCs. Taken together, these

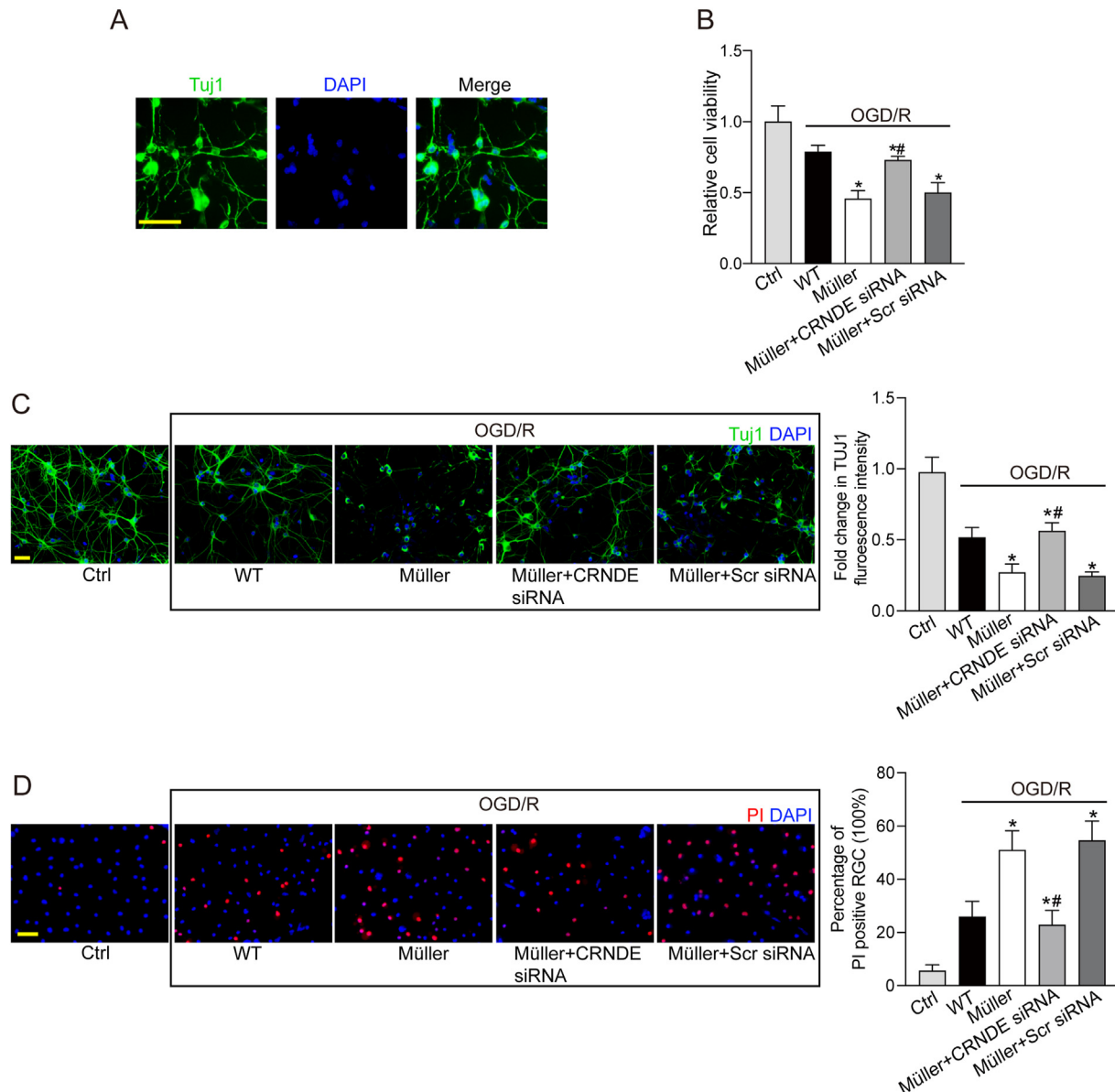


Figure 6. LncRNA-CRNDE knockdown indirectly regulates RGC function after OGD/R *in vitro*. Primary RGCs were co-cultured with Müller cells. Müller cells were transfected with lncRNA-CRNDE siRNA or Scr siRNA or left untreated (WT), and then the experimental groups were exposed to OGD (6 h)/R (12 h). A. Primary RGCs were confirmed with retinal ganglion cell marker Tuj1 antibody. Blue, DAPI; Green, Tuj1 (Scale bar: 20 μ m). B. MTT assay and quantification analysis were performed to detect the viability of RGCs ($n = 4$). $*P < 0.05$ versus Ctrl, $\#P < 0.05$ OGD/R + Müller + CRNDE siRNA versus OGD/R + Müller + Scr siRNA. The significant difference was determined by one-way ANOVA followed by Bonferroni test. C. Immunofluorescent staining and quantification analysis were confirmed to detect the synaptic morphology of RGCs. Blue, DAPI; Green, Tuj1 ($n = 4$; Scale bar: 20 μ m). $*P < 0.05$ versus Ctrl, $\#P < 0.05$ OGD/R + Müller + CRNDE siRNA versus OGD/R + Müller + Scr siRNA. The significant difference was determined by one-way ANOVA followed by Bonferroni test. D. PI staining and quantitative analysis were performed to detect the dead or dying RGCs ($n = 4$; Scale bar: 50 μ m). $*P < 0.05$ versus Ctrl, $\#P < 0.05$ OGD/R + Müller + CRNDE siRNA versus OGD/R + Müller + Scr siRNA. The significant difference was determined by one-way ANOVA followed by Bonferroni test.

results indicate that lncRNA-CRNDE may be a crucial regulator of Müller cell function and has an indirect effect on RGC function *in vitro*.

3.4. lncRNA-CRNDE causes a noteworthy change in cytokine profile *in vivo*

As is well known to us all, the balance of reactive glial cells is important for neuron survival as reactive glial cells can produce growth factors and immunomodulatory cytokines [25]. To determine whether lncRNA-CRNDE regulates glial cell reactivity and affects cytokine release, we detected the cytokine profile of the lysates from RIR-injured retinas and lncRNA-CRNDE shRNA-injected RIR-injured retinas via qRT-PCR and ELISA assays. We observed clearly from qRT-PCR array that lncRNA-CRNDE knockdown resulted in a significant reduction in the amount of three mRNAs, namely, ICAM-1, TNF- α , and IL-6 (Figure 7A). ELISA assays also showed that lncRNA-CRNDE silencing reduced retinal inflammation (Figure 7B). These data suggest that the increased secretion of pro-inflammatory factors in the retinas might be one of the mechanisms of RIR injury.

4. Discussion

lncRNAs are involved in regulating important biological processes, including genomic imprinting, dosage compensation (e.g., X chromosome inactivation), regulation of the cell cycle, and the differentiation and development programs of somatic cells [26]. Multiple research studies have highlighted the importance of lncRNAs dysregulation in human disorders, including cancer, and cardiac and neurodegenerative disorders [27]. As an oncogene, lncRNA-CRNDE is highly expressed in hypoxic-ischemic brain damage, lncRNA-CRNDE silencing alleviates hypoxic-ischemic brain damage, at least partially, through promoting autophagy [13]. This study shows that lncRNA-CRNDE expression levels are significantly up-regulated in the retinas following ischemia-reperfusion (IR) and in Müller cells upon hyperoxia stress. lncRNA-CRNDE knockdown decreases Müller cell over-activation and increases RGC survival *in vivo* and *in vitro*. This study may provide a novel insight for investigating the role of lncRNA-CRNDE in neurodegeneration induced by RIR injury and provides a promising target for preventing retinal neurodegeneration in RIR.

RIR injury is a common pathological process in various ocular diseases, including diabetic retinopathy, retinal vascular occlusion, anterior optic neuropathy, and glaucoma [28]. Therapies that delay or halt the loss of RGCs have been proven effective in preserving the vision of patients with

glaucoma [14]. In this study, the ocular hypertension-induced RIR injury model has been used to investigate the pathogenesis of neurodegenerative diseases and explore new neuroprotective therapies. We demonstrate that lncRNA-CRNDE knockdown could significantly reduce the percentage of apoptotic retinal cells and alleviate RIR injury. Moreover, a retinal electrophysiology assay showed that lncRNA-CRNDE knockdown improved visual function after RIR injury. Thus, these results suggest that lncRNA-CRNDE is involved in regulating RIR-induced retinal neurodegeneration *in vivo*.

Glial cells provide structural and metabolic support to retinal neurons and become reactive in response to external stresses [29]. Müller cells are the most abundant glial cells in the retina that span the entire thickness of the retina [30]. They constitute an anatomical and functional link with retinal neurons and contribute to intraretinal homeostasis. Under the pathological condition, including photic damage, retinal trauma, ischemia, glaucoma and diabetic retinopathy, Müller cells exhibit nonspecific gliotic responses. Reactive gliosis includes cell proliferation, changes in cell shape, and upregulation of the intermediate filament system [31]. However, repetitive pathological stimulation exacerbates the proliferation of Müller cells, causing cell dysfunction, damaging photoreceptor cells, and neurons, leading to glial scars, inhibiting retinal remodeling, and limiting the ability to regenerate damaged retinal tissue, eventually leading to blindness [32]. As a result, we performed the MTT assay, EdU staining, and PI/Calcein-AM staining to examine the role of lncRNA-CRNDE in Müller cell function. Results showed that lncRNA-CRNDE knockdown significantly reduces Müller glial cell viability, decreases the proliferation of Müller glial cells, and promotes the apoptosis of Müller glial cells induced by OGD/R. In addition, lncRNA-CRNDE knockdown decreases GFAP and GS expression in the retina induced by RIR injury *in vivo*. Thus, it is not surprising that lncRNA-CRNDE is involved in the pathological process of RIR injury.

A previous study showed a close relationship between Müller cells and RGCs in RIR injury [33]. In addition, our previous study showed the Müller cells are activated after STZ-induced diabetes, while suppressing the active Müller cells by AQP4-AS1 knockdown could improve the survival of RGCs [34]. RGC death in glaucoma and neural degeneration models is associated with accumulation of activated glia, and inhibition of Müller glia and astrocytes result in an increase in RGCs [35, 36, 37, 38]. Müller cells are among the first responders following intraocular pressure increase. Studies of the DBA/2J mouse model of glaucoma and episcleral vein cauterization-induced glaucoma rat model suggest that Müller cell hypertrophy and activation were detected at the early stages of glaucoma (as early as 2–3 days), preceding detectable RGC disease

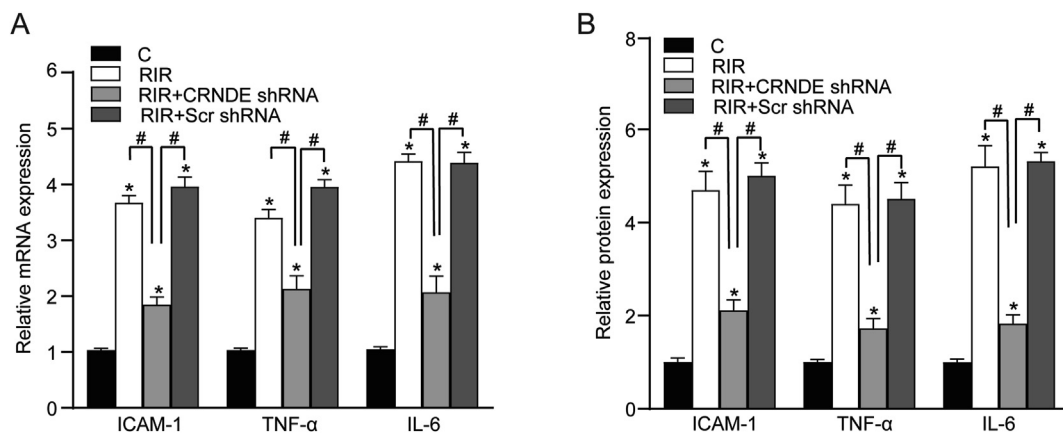


Figure 7. lncRNA-CRNDE knockdown regulates the level of inflammatory factor after RIR. lncRNA-CRNDE knockdown causes a significant change in inflammatory factor *in vivo*. C57BL/6J mice (4-week-old, male) received an intravitreal injection of Scr shRNA or lncRNA-CRNDE shRNA or left untreated. Four weeks after shRNA injection, RIR was induced. The group without RIR served as the control (Ctrl) group. A. qRT-PCR assays were conducted to determine the relative levels of ICAM-1, TNF- α and ICAM-1mRNA ($n = 3$). $*P < 0.05$, $\#P < 0.05$ RIR + CRNDE versus RIR and RIR + Scr, the significant difference was determined by one-way ANOVA followed by Bonferroni test. B. ELISA was conducted to detect the relative protein expression of ICAM-1, TNF- α and ICAM-1. A representative immunoblot is shown along with the quantitative data ($n = 4$). $*P < 0.05$, $\#P < 0.05$ RIR + CRNDE versus RIR and RIR + Scr, the significant difference was determined by one-way ANOVA followed by Bonferroni test.

[39, 40]. Reactive Müller glia could increase the susceptibility of RGCs to stress signals by releasing neurotoxic factors and contribute to disease progression [41]. Thus, modulation of Müller cell responses may alter disease progression. It is known that the presence and distribution of retinal astrocytes are correlated with the density of the nerve fibers that they ensheath and the presence of retina blood vessels [42]. As the main producers of VEGF, astrocytes are implicated in retinal vascularization and vascular mediation. However, the transformation of surveying astrocytes into alerted or reactive states, in response to a perceived threat, could have a detrimental effect on RGCs axons via secretion of proinflammatory cytokines such as IL-6, TNF- α , and nitric oxide [43, 44, 45]. In our results, the number of apoptotic RGCs was significantly increased after OGD/R treatment, as in those co-cultured with Müller cells, compared with those that were not co-culture with Müller cells. Furthermore, lncRNA-CRNDE knockdown in Müller cells significantly reduced the damaging effect on the co-cultured RGCs in response to OGD/R. These studies show that lncRNA-CRNDE knockdown could indirectly protect the RGCs after OGD/R *in vitro*. Consistently, *in vivo* studies reveal that the lncRNA-CRNDE knockdown group has more RGC survival than the Scr shRNA-injected group after RIR.

When tissues are exposed to ischemia followed by reperfusion, ROS are extensively generated in the early reperfusion stage. ROS could cause heavy damage to the retina [46]. Moreover, increasing evidence demonstrates that oxidative stress induced by ROS plays a key role in the pathophysiological mechanisms in RIR injury [47]. Interestingly, RIR injury could induce the production of a variety of inflammatory mediators in the retina, including IL-1 β , ICAM-1, and IL-6 [48]. Oxidative stress was found to be involved in the production of these inflammatory mediators and is now considered as one of the most important factors that mediate the process of apoptosis [49]. lncRNA-CRNDE knockdown inhibited the expression of IL-1 β , ICAM-1, and IL-6 in the retina induced by RIR injury. These results suggest that lncRNA-CRNDE plays an important role in the pathological process of RIR injury by regulating the release of immunomodulatory cytokines.

In conclusion, this study reveals the role of lncRNA-CRNDE in RIR injury. lncRNA-CRNDE directly regulates the biological functions of Müller cells and indirectly regulates the functions of RGCs. These findings indicate that lncRNA-CRNDE is involved in retinal neurodegeneration dysfunction. Furthermore, mechanistically, lncRNA-CRNDE silencing inhibits the release of immunomodulatory cytokines, alleviating RIR-induced neurodegeneration dysfunction. Collectively, this study suggests that lncRNA-CRNDE is a promising target for the prevention of retinal neurodegeneration complications.

Declarations

Author contribution statement

Ting-Ting Sun: Conceived and designed the experiments; Performed the experiments; Analyzed and interpreted the data; Wrote the paper.

Xiu-Miao Li, Jun-Ya Zhu, Wen Yao and Tian-Jing Yang: Performed the experiments; Analyzed and interpreted the data; Wrote the paper.

Xiang-Rui Meng: Performed the experiments; Analyzed and interpreted the data.

Jin Yao and Qin Jiang: Conceived and designed the experiments; Contributed reagents, materials, analysis tools or data; Wrote the paper.

Funding statement

Qin Jiang, Jin Yao, Mr Qin Jiang, Xiu-Miao Li were supported by National Natural Science Foundation of China (81870679, 81970823, 82070983, 81800858) respectively.

Data availability statement

Data will be made available on request.

Declaration of interests statement

The authors declare no conflict of interest.

Additional information

No additional information is available for this paper.

Acknowledgements

Not applicable.

References

- [1] B.J. Kim, T.A. Braun, R.J. Wordinger, A.F. Clark, Progressive morphological changes and impaired retinal function associated with temporal regulation of gene expression after retinal ischemia/reperfusion injury in mice, *Mol Neurodegener* 8 (2013) 21.
- [2] J.L. Ang, S. Ah-Moye, L.N. Kim, V. Nguyen, A. Hunt, D. Barthelmes, et al., A systematic review of real-world evidence of the management of macular oedema secondary to branch retinal vein occlusion, *Eye (Lond)* 34 (10) (2020) 1770–1796.
- [3] D. Zur, M. Iglicki, A. Loewenstein, The role of steroids in the management of diabetic macular edema, *Ophthalmic Res* 62 (4) (2019) 231–236.
- [4] H.K. Eltzschig, T. Eckle, Ischemia and reperfusion—from mechanism to translation, *Nat Med* 17 (11) (2011) 1391–1401.
- [5] B. Mathew, S. Ravindran, X. Liu, L. Torres, M. Chennakesavalu, C.C. Huang, et al., Mesenchymal stem cell-derived extracellular vesicles and retinal ischemia-reperfusion, *Biomaterials* 197 (2019) 146–160.
- [6] M. Kawaguchi, M. Takahashi, T. Hata, Y. Kashima, F. Usui, H. Morimoto, et al., Inflammasome activation of cardiac fibroblasts is essential for myocardial ischemia/reperfusion injury, *Circulation* 123 (6) (2011) 594–604.
- [7] Y. Yang, V.M. Salayandia, J.F. Thompson, L.Y. Yang, E.Y. Estrada, Y. Yang, Attenuation of acute stroke injury in rat brain by minocycline promotes blood-brain barrier remodeling and alternative microglia/macrophage activation during recovery, *J Neuroinflammation* 12 (2015) 26.
- [8] F. Kopp, J.T. Mendell, Functional classification and experimental dissection of long noncoding RNAs, *Cell* 172 (3) (2018) 393–407.
- [9] L.K. Wang, X.F. Chen, D.D. He, Y. Li, J. Fu, Dissection of functional lncRNAs in Alzheimer's disease by construction and analysis of lncRNA-mRNA networks based on competitive endogenous RNAs, *Biochem Biophys Res Commun* 485 (3) (2017) 569–576.
- [10] H.K. Choe, J. Cho, Comprehensive genome-wide approaches to activity-dependent translational control in neurons, *Int J Mol Sci* 21 (5) (2020) 1592.
- [11] L.D. Graham, S.K. Pedersen, G.S. Brown, T. Ho, Z. Kassir, A.T. Moynihan, et al., Colorectal neoplasia differentially expressed (CRNDE), a novel gene with elevated expression in colorectal adenomas and adenocarcinomas, *Genes Cancer* 2 (8) (2011) 829–840.
- [12] S.W. Shahab, L.V. Matyunina, R. Mezencev, L.D. Walker, N.J. Bowen, B.B. Benigno, et al., Evidence for the complexity of microRNA-mediated regulation in ovarian cancer: a systems approach, *PLoS One* 6 (7) (2011), e22508.
- [13] C.H. Fu, F.F. Lai, S. Chen, C.X. Yan, B.H. Zhang, C.Z. Fang, et al., Silencing of long non-coding RNA CRNDE promotes autophagy and alleviates neonatal hypoxic-ischemic brain damage in rats, *Mol. Cell. Biochem.* 472 (1–2) (2020) 1–8.
- [14] P. Wan, W. Su, Y. Zhang, Z. Li, C. Deng, Y. Zhuo, Trimetazidine protects retinal ganglion cells from acute glaucoma via the Nrf2/Ho-1 pathway, *Clin. Sci. (Lond.)* 131 (18) (2017) 2363–2375.
- [15] E. Shosha, Z. Xu, H. Yokota, A. Saul, M. Rojas, R.W. Caldwell, et al., Arginase 2 promotes neurovascular degeneration during ischemia/reperfusion injury, *Cell Death Dis.* 7 (11) (2016), e2483.
- [16] K.J. Livak, T.D. Schmittgen, Analysis of relative gene expression data using real-time quantitative PCR and the 2(-Delta Delta C(T)) Method, *Methods* 25 (4) (2001) 402–408.
- [17] S.A. Nair, R.K. Sr, A.S. Nair, S. Baby, Citrus peels prevent cancer, *Phytomedicine* 50 (2018) 231–237.
- [18] X. Zhu, S. Li, C. Huang, G. Huang, J. Xu, lncRNA CRNDE inhibits cardiomyocytes apoptosis by YAP1 in myocardial ischaemia/reperfusion injury, *Autoimmunity* 54 (4) (2021) 204–212.
- [19] H. Chen, Y. Deng, X. Gan, Y. Li, W. Huang, L. Lu, et al., NLRP12 collaborates with NLRP3 and NLR4 to promote pyroptosis inducing ganglion cell death of acute glaucoma, *Mol. Neurodegener.* 15 (1) (2020) 26.
- [20] E. Rungger-Brändle, A.A. Dosso, P.M. Leuenberger, Glial reactivity, an early feature of diabetic retinopathy, *Invest. Ophthalmol. Vis. Sci.* 41 (7) (2000) 1971–1980.
- [21] M.H. Madeira, R. Boia, P.F. Santos, A.F. Ambrosio, A.R. Santiago, Contribution of microglia-mediated neuroinflammation to retinal degenerative diseases, *Mediat. Inflamm.* (2015) 673090.
- [22] A.E. Koh, H.A. Alsaedi, M.B.A. Rashid, C. Lam, M.H.N. Harun, M. Saleh, et al., Retinal degeneration rat model: a study on the structural and functional changes in the retina following injection of sodium iodate, *J. Photochem. Photobiol., B* 196 (2019) 111514.
- [23] H. Ding, R.G. Smith, A. Poleg-Polsky, J.S. Diamond, K.L. Briggman, Species-specific wiring for direction selectivity in the mammalian retina, *Nature* 535 (7610) (2016) 105–110.
- [24] F. Soto, N.W. Tien, A. Goel, L. Zhao, P.A. Ruzycski, D. Kerschensteiner, AMIGO2 scales dendrite arbors in the retina, *Cell Rep.* 29 (6) (2019) 1568–1578.

- [25] A. Rübsam, S. Parikh, P.E. Fort, Role of inflammation in diabetic retinopathy, *Int. J. Mol. Sci.* 19 (4) (2018).
- [26] T.R. Mercer, J.S. Mattick, Structure and function of long noncoding RNAs in epigenetic regulation, *Nat. Struct. Mol. Biol.* 20 (3) (2013) 300–307.
- [27] I.A. Qureshi, J.S. Mattick, M.F. Mehler, Long non-coding RNAs in nervous system function and disease, *Brain Res.* 1338 (2010) 20–35.
- [28] M. Vidal-Sanz, M. Salinas-Navarro, F.M. Nadal-Nicolás, L. Alarcón-Martínez, F.J. Valiente-Soriano, J.M. De Imperial, et al., Understanding glaucomatous damage: anatomical and functional data from ocular hypertensive rodent retinas, *Prog. Retin. Eye Res.* 31 (1) (2012) 1–27.
- [29] A. Bringmann, T. Pannicke, B. Biedermann, M. Francke, I. Iandiev, J. Grosche, et al., Role of retinal glial cells in neurotransmitter uptake and metabolism, *Neurochem. Int.* 54 (3–4) (2009) 143–160.
- [30] A. Bringmann, T. Pannicke, J. Grosche, M. Francke, P. Wiedemann, S.N. Skatchkov, et al., Müller cells in the healthy and diseased retina, *Prog. Retin. Eye Res.* 25 (4) (2006) 397–424.
- [31] A. Bringmann, I. Iandiev, T. Pannicke, A. Wurm, M. Hollborn, P. Wiedemann, et al., Cellular signaling and factors involved in Müller cell gliosis: neuroprotective and detrimental effects, *Prog. Retin. Eye Res.* 28 (6) (2009) 423–451.
- [32] M. Pekny, M. Nilsson, Astrocyte activation and reactive gliosis, *Glia* 50 (4) (2005) 427–434.
- [33] G. Edenfeld, T. Stork, C. Klämbt, Neuron-glia interaction in the insect nervous system, *Curr. Opin. Neurobiol.* 15 (1) (2005) 34–39.
- [34] X. Li, J. Zhu, Y. Zhong, C. Liu, M. Yao, Y. Sun, et al., Targeting long noncoding RNA-AQP4-AS1 for the treatment of retinal neurovascular dysfunction in diabetes mellitus, *EBioMedicine* 77 (2022) 103857.
- [35] H. Tawarayama, M. Inoue-Yanagimachi, N. Himori, T. Nakazawa, Glial cells modulate retinal cell survival in rotenone-induced neural degeneration, *Sci. Rep.* 11 (1) (2021) 11159.
- [36] M.S. Sung, H. Heo, G.H. Eom, S.Y. Kim, H. Piao, Y. Guo, et al., HDAC2 regulates glial cell activation in ischemic mouse retina, *Int. J. Mol. Sci.* 20 (20) (2019).
- [37] R. Huang, Q. Lan, L. Chen, H. Zhong, L. Cui, L. Jiang, et al., CD200Fc attenuates retinal glial responses and RGCs apoptosis after optic nerve crush by modulating CD200/CD200R1 interaction, *J. Mol. Neurosci.* 64 (2) (2018) 200–210.
- [38] N. Li, F. Wang, Q. Zhang, M. Jin, Y. Lu, S. Chen, et al., Rapamycin mediates mTOR signaling in reactive astrocytes and reduces retinal ganglion cell loss, *Exp. Eye Res.* 176 (2018) 10–19.
- [39] A. Kanamori, M. Nakamura, Y. Nakanishi, Y. Yamada, A. Negi, Long-term glial reactivity in rat retinas ipsilateral and contralateral to experimental glaucoma, *Exp. Eye Res.* 81 (1) (2005) 8–56.
- [40] D.M. Inman, P.J. Horner, Reactive nonproliferative gliosis predominates in a chronic mouse model of glaucoma, *Glia* 55 (9) (2007) 942–953.
- [41] Y. Bai, D. Sivori, S.B. Woo, K.E. Neet, S.F. Lerner, H.U. Saragovi, During glaucoma, alpha2-macroglobulin accumulates in aqueous humor and binds to nerve growth factor, neutralizing neuroprotection, *Invest. Ophthalmol. Vis. Sci.* 52 (8) (2011) 5260–5265.
- [42] T. Watanabe, M.C. Raff, Retinal astrocytes are immigrants from the optic nerve, *Nature* 332 (6167) (1988) 834–837.
- [43] E.C. Johnson, T.A. Doser, W.O. Cepurna, J.A. Dyck, L. Jia, Y. Guo, et al., Cell proliferation and interleukin-6-type cytokine signaling are implicated by gene expression responses in early optic nerve head injury in rat glaucoma, *Invest. Ophthalmol. Vis. Sci.* 52 (1) (2011) 504–518.
- [44] L. Yuan, A.H. Neufeld, Tumor necrosis factor-alpha: a potentially neurodestructive cytokine produced by glia in the human glaucomatous optic nerve head, *Glia* 32 (1) (2000) 42–50.
- [45] M. Almasieh, A.M. Wilson, B. Morquette, J.L. Cueva Vargas, A. Di Polo, The molecular basis of retinal ganglion cell death in glaucoma, *Prog. Retin. Eye Res.* 31 (2) (2012) 152–181.
- [46] G. Gutiérrez-Sánchez, I. García-Alonso, J. Gutiérrez Sáenz De Santa María, A. Alonso-Varona, B. Herrero De La Parte, Antioxidant-Based Therapy Reduces Early-Stage Intestinal Ischemia-Reperfusion Injury in Rats, *Antioxidants (Basel)* 10 (6) (2021).
- [47] K. Kovacs, A. Vaczy, K. Fekete, P. Kovari, T. Atlasz, D. Reglodi, et al., PARP inhibitor protects against chronic hypoxia/reoxygenation-induced retinal injury by regulation of MAPKs, HIF1 α , Nrf2, and NF κ B, *Invest Ophthalmol Vis Sci* 60 (5) (2019) 1478–1490.
- [48] H. Luo, J. Zhuang, P. Hu, W. Ye, S. Chen, Y. Pang, et al., Resveratrol delays retinal ganglion cell loss and attenuates gliosis-related inflammation from ischemia-reperfusion injury, *Invest Ophthalmol Vis Sci* 59 (10) (2018) 3879–3888.
- [49] Y. Li, X. Ren, C. Lio, W. Sun, K. Lai, Y. Liu, et al., A chlorogenic acid-phospholipid complex ameliorates post-myocardial infarction inflammatory response mediated by mitochondrial reactive oxygen species in SAMP8 mice, *Pharmacol. Res.* 130 (2018) 110–122.